



## Decreased subunit exchange of heat-treated lens $\alpha$ A-crystallin

Jack J.-N. Liang\* and Ling Fu

*Department of Ophthalmology, Center for Ophthalmic Research, Brigham and Women's Hospital, Harvard Medical School,  
221 Longwood Avenue, Boston, MA 02115, USA*

Received 8 March 2002

### Abstract

$\alpha$ A-Crystallin high-molecular-weight (HMW) aggregates were prepared by preheating at 80–90 °C and studied using spectroscopic measurements. Conformational differences were suggested based on data of increased bis-ANS (4,4'-dianilino-1,1'-binaphthalene-5,5'-disulfonic acid) and ThT (thioflavin T) fluorescence as well as increased far-UV and decreased near-UV circular dichroism (CD). These results indicated that HMW aggregated  $\alpha$ -crystallin was more hydrophobic than the native  $\alpha$ -crystallin, possibly resulting from partial unfolding of  $\alpha$ -crystallin. The two cysteines in  $\alpha$ A-crystallin were mostly oxidized in HMW aggregates. The effects of HMW aggregation on the dynamic structure were studied with fluorescence resonance energy transfer; subunit exchange became slower. These results strongly suggest that HMW  $\alpha$ A-crystallin aggregates result from exposure of buried  $\beta$ -pleated sheets and increased hydrophobic interaction. © 2002 Elsevier Science (USA). All rights reserved.

**Keywords:**  $\alpha$ A-Crystallin; Circular dichroism; Fluorescence resonance energy transfer; High-molecular-weight aggregation; Subunit exchange

Lens  $\alpha$ -crystallin normally exists as an oligomer with a molecular weight of 600–800 kDa and aggregates to a high-molecular-weight (HMW) protein in vivo with age and cataract formation [1]. The oligomeric  $\alpha$ -crystallin consists of two subunits,  $\alpha$ A- and  $\alpha$ B-crystallins with a ratio of 3 to 1 in most mammalian lenses. HMW aggregates can also be induced in vitro by heating at high temperatures [2–5]. The mechanisms of HMW aggregation are not fully established, and it is also not known whether the in vivo and in vitro HMW aggregations share the same mechanisms. Based on some spectroscopic studies, we speculated that the mechanisms involved partial unfolding [2,3]. Although in vitro heating-induced aggregation is nonphysiological, it provides a convenient way to study the mechanisms of HMW aggregation. We have reported that some spectroscopic properties of in vitro HMW aggregates are similar to those of in vivo HMW aggregates [6]. In the present study, HMW aggregates were isolated from preheated  $\alpha$ A-crystallin and the effects of aggregation on conformation and function were studied by spectroscopic measurements.

One unique property of  $\alpha$ -crystallin is its possession of dynamic structure; subunits are constantly undergoing exchange, which has been suggested to be responsible for some properties of  $\alpha$ -crystallin, such as stability [7,8]. Subunit exchange has been studied by methods of native IEF and fluorescence resonance energy transfer (FRET) [7–10]. HMW aggregated  $\alpha$ -crystallin may not readily participate in subunit exchange and thus may show impaired function. In aged and cataractous lenses, a large amount of HMW aggregated  $\alpha$ -crystallin was observed. It is speculated that these HMW aggregates have a reduced subunit exchange with LMW  $\alpha$ -crystallin, which makes them functionally less stable.

### Materials and methods

**Recombinant  $\alpha$ A-crystallin.** Cloning and expression of  $\alpha$ A-crystallin and W9F mutant are described elsewhere [10,11].  $\alpha$ A-Crystallin has one Trp-9 and was substituted with Phe in the W9F mutant [10].

$\alpha$ A-Crystallin samples (0.2–0.5 mg/mL) in 50 mM phosphate buffer, pH 7.4, were preheated at 80 or 90 °C for 1 h. Aggregation was detected by FPLC gel filtration with a Superose-6 column. The amount of HMW aggregates eluting at void volume increased with heating time or temperature (see Fig. 1). After heating at 90 °C for 1 h, most  $\alpha$ A-crystallin was in the aggregated state. The fractions of the aggregated state of  $\alpha$ A-crystallin with molecular size >2000 kDa (void volume) were collected and used for the present comparative study.

\* Corresponding author. Fax: +1-617-278-0556.

E-mail address: jliang@rics.bwh.harvard.edu (J.J.-N. Liang).

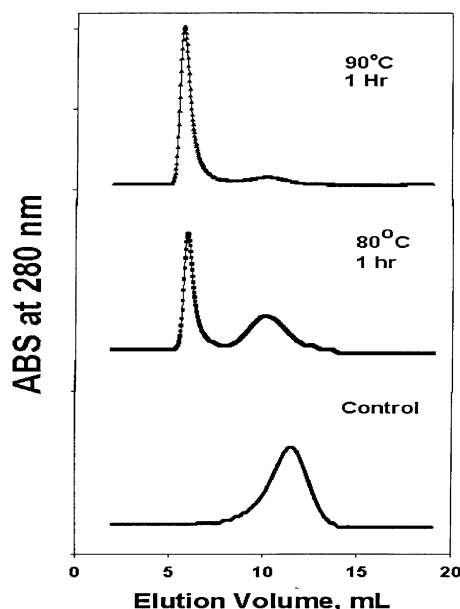


Fig. 1. FPLC gel filtration FPLC of  $\alpha$ A-crystallin preheated at 80 or 90 °C for 1 h. Flow rate was 0.5 mL/min and 1-mL fractions were collected.

SDS-PAGE was performed in a slab gel (15% acrylamide) under both reducing and nonreducing conditions. Protein concentrations were determined by the Pierce BCA protein assay, with BSA as a standard [12]. Absorption at 280 nm increased for the HMW  $\alpha$ A-crystallin, possibly due to disulfide formation (see Fig. 3) and light scattering; estimation of protein concentration by extinction coefficient is not appropriate.

**CD measurements.** CD spectra were measured with an Aviv Circular Dichroism Spectrometer (Model 60 DS; AVIV, Lakewood, NJ). Five scans were averaged and smoothed by a polynomial-fitting program. The CD intensity is expressed as molar ellipticity with unit of  $\text{deg cm}^2 \text{dmol}^{-1}$ .

**Fluorescence measurements.** Fluorescence was measured with an RF-5301PC Shimadzu Spectrofluorometer (Shimadzu, Columbia, MD). Trp fluorescence spectra were obtained with excitation wavelengths of 295 nm. Bis-ANS (4,4'-dianilino-1,1'-binaphthalene-5,5'-disulfonic acid;  $\epsilon = 23 \times 10^3 \text{ cm}^{-1} \text{ M}^{-1}$  at 395 nm) (Molecular Probes, Junction City, OR) and ThT (thioflavin T;  $\epsilon = 26.62 \times 10^3 \text{ cm}^{-1} \text{ M}^{-1}$  at 416 nm) (Sigma Chemicals, St. Louis, MO) were used to probe the change in hydrophobicity and  $\beta$ -sheet conformation, with excitation wavelength at 395 and 450 nm, respectively. Aliquots (20  $\mu\text{L}$ ) of bis-ANS stock solution ( $4.5 \times 10^{-4} \text{ M}$ ) or ThT stock solution (3.5  $\mu\text{M}$ ) were added to 1 mL of protein samples and allowed to sit at room temperature for 15 min before measurement. The titration was continued until saturation was reached.

The status of cysteine was determined by MIANS fluorescence [2-(4'-maleimidyl)anilino] naphthalene-6-sulfonic acid] (MIANS,  $\epsilon = 27 \times 10^3 \text{ cm}^{-1} \text{ M}^{-1}$  at 322 nm) (Molecular Probes, Junction City, OR). At pH 7–7.6, MIANS binds only to SH groups. Excess MIANS (in molar ratio) was added to the protein solution. MIANS fluorescence arises only after binding with a protein; it does not give any fluorescence in phosphate buffer.

**Subunit exchange study.** For the subunit exchange study, the Trp-deficient W9F mutant was similarly treated with MIANS as in the determination of cysteine. The excess MIANS was removed by dialysis. The degree of labeling was approximately 1.4 mol of MIANS per mole of  $\alpha$ A-crystallin W9F. The MIANS-labeled W9F mutant was mixed with either WT or HMW aggregated  $\alpha$ A-crystallin. The mixtures were

subjected to FRET measurements at 37 °C at intervals of 15–60 min for 6–7 h. The labeled MIANS acts as an acceptor with an excitation wavelength at 322 nm, which overlaps with emission of the donor Trp (emission between 310 and 350 nm). When the two probes were in a close proximity resulting from intermolecular reaction, energy transfer would occur. The emission scanning ( $\lambda_{\text{ex}} = 290 \text{ nm}$ ) will show a decrease of Trp fluorescence intensity and an increase of MIANS fluorescence intensity with time. The exchange rate is dependent upon many parameters, such as temperature, ionic strength, etc. [9,10] and in the present study the temperature of 37 °C was chosen. The efficiency of energy transfer ( $E$ ) is calculated with the equation  $E = 1 - (F_t/F_0)$ , where  $F_t$  and  $F_0$  are emission intensities of donor at time  $t$  and 0, respectively. The efficiency depends on the inverse sixth power of the distance between donor and acceptor and the critical distance for energy transfer is in the range of 20–50 Å [13]. Since the size of  $\alpha$ -crystallin aggregates is 150–200 Å, the measurements provide a sensitive detection of either intermolecular exchange or interaction [10].

## Results

### HMW aggregates

Fig. 1 shows the elution pattern of wild-type  $\alpha$ A-crystallin preheated at 80 or 90 °C for 1 h. The fractions at void volume ( $>2000 \text{ kDa}$ ) increased with duration or increasing temperatures and those with 1 h heating at 80 °C were collected as HMW aggregated  $\alpha$ A-crystallin. The exact molecular weight of HMW  $\alpha$ A-crystallin is not known but is not important in the present study.

SDS-PAGE patterns in the presence and absence of  $\beta$ -mercaptoethanol are shown in Fig. 2. Less staining for HMW aggregates was observed as reported previously [6]. Increasing amount of disulfide cross-linked dimer

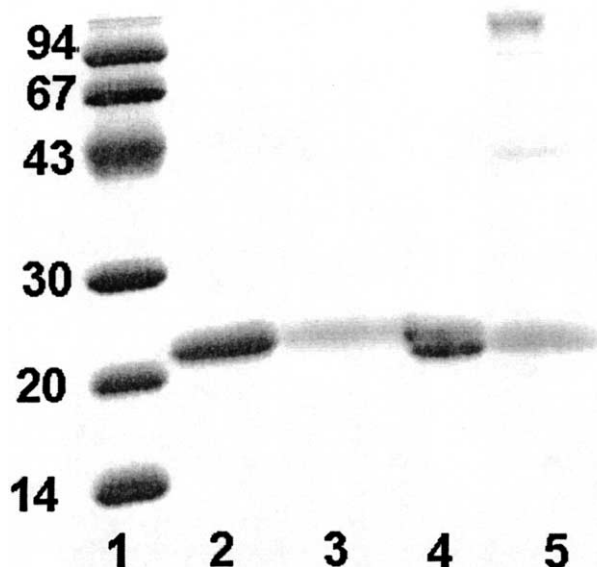


Fig. 2. SDS-PAGE patterns of native and HMW  $\alpha$ A-crystallins: Lane 1, MW marker; lanes 2 and 4, native form; lanes 3 and 5, HMW aggregated form. Lanes 2 and 3 were run under reducing conditions and lanes 4 and 5 were run under nonreducing conditions.

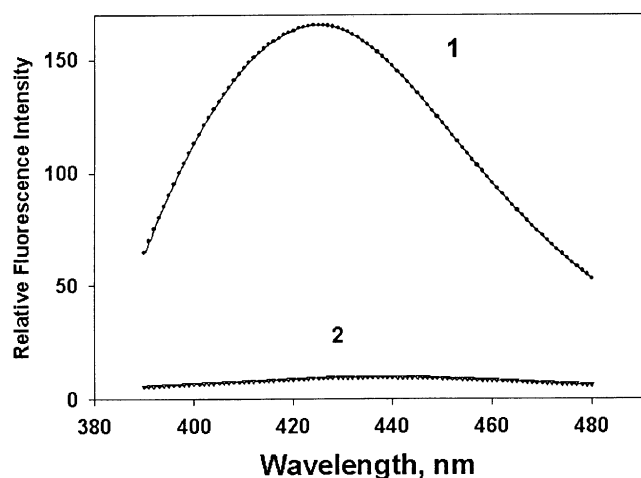


Fig. 3. MIANS fluorescence spectra of native (curve 1) and HMW aggregated (curve 2)  $\alpha$ A-crystallins: Excitation wavelength was 322 nm. Protein concentration was 0.1 mg/mL in 50 mM phosphate buffer, pH 7.4.

and trimer species was observed in the HMW aggregates. The change of cysteine is further confirmed by MIANS fluorescence as shown in Fig. 3. A large decreased intensity was observed for HMW  $\alpha$ A-crystallin. MIANS fluorescence intensity correlates closely with the hydrophobic environment of Cys groups [14,15] and the observed decrease is due mainly to disulfide formation rather than the inaccessibility of Cys groups. The latter will show a blue shift of emission wavelength rather than a decrease in intensity.

#### Circular dichroism

Fig. 4 shows the far-UV and near-UV CD of HMW and native  $\alpha$ A-crystallin. The characteristic 215–218 nm band of  $\beta$ -pleated sheet was shifted to 208 nm, which seems to be an indication of increase of  $\alpha$ -helical content. But the secondary structural analysis indicated no increase in  $\alpha$ -helical content, rather an increase of  $\beta$ -pleated sheet was observed. The percentage of secondary structures for the control  $\alpha$ A-crystallin was found to be 8, 40, 24, and 29, respectively, for  $\alpha$ -helix,  $\beta$ -pleated sheet,  $\beta$  turn, and random coil. The corresponding figures for HMW  $\alpha$ A-crystallin were 8, 48, 11, and 34, respectively. The exact content of each secondary structure may vary from the reported values [16–18], but the important observation was that heat-treatment did not completely denature  $\alpha$ A-crystallin, which is further supported by Trp fluorescence (see below).

Near-UV CD bands for HMW  $\alpha$ -crystallin were shifted towards more negative. This change was very similar to that in heat-induced HMW aggregation of bovine lens  $\alpha$ -crystallin [2]. Such a result is usually caused by partial unfolding and aggregation.

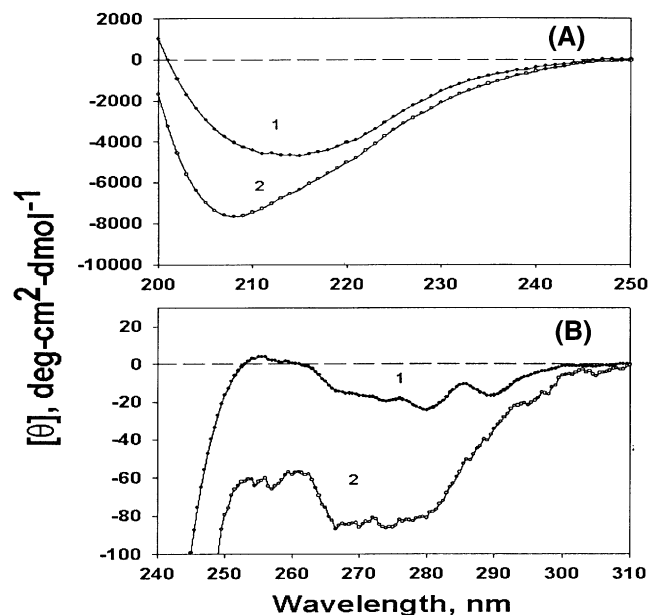


Fig. 4. (A) Far-UV CD and (B) near-UV CD spectra of native (curve 1) and HMW (curve 2)  $\alpha$ A-crystallins. Protein concentration was 0.1 mg/mL in 50 mM phosphate buffer, pH 7.4, and cell path-lengths were 1 mm for far-UV CD and 0.5 mg/mL and 10 mm for near-UV CD measurements. The spectra were an average of five scans smoothed by a polynomial-fitting program.

#### Fluorescence

Trp fluorescence shows little shift in emission maximum wavelength ( $\lambda_{em} = 336$ –337 nm) for HMW aggregates (Fig. 5). Similar treatment of  $\beta$ B2-crystallin generated a partially unfolded protein ( $\lambda_{em}$  shifted from 331 to 339 nm) [19].

Large increases of bis-ANS and ThT fluorescence intensity for HMW aggregates were observed (Figs. 6A

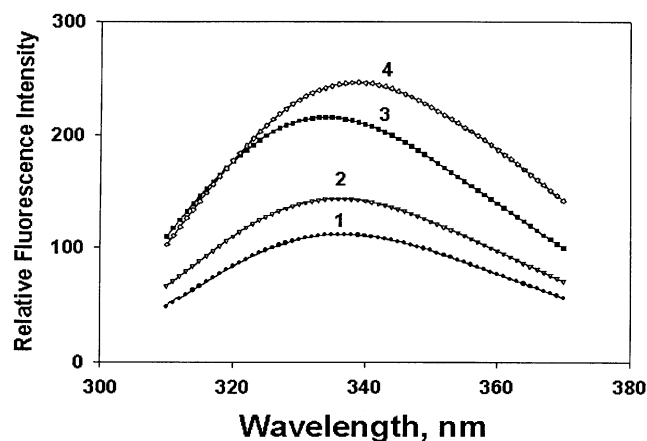


Fig. 5. Trp fluorescence spectra of native (curve 1) and HMW (curve 2) aggregated  $\alpha$ A-crystallins: Curves 3 and 4 are the corresponding spectra for the control and preheated  $\beta$ B2-crystallin for comparison. Excitation wavelength was 295 nm and protein concentration was 0.1 mg/mL in 50 mM phosphate buffer, pH 7.4.

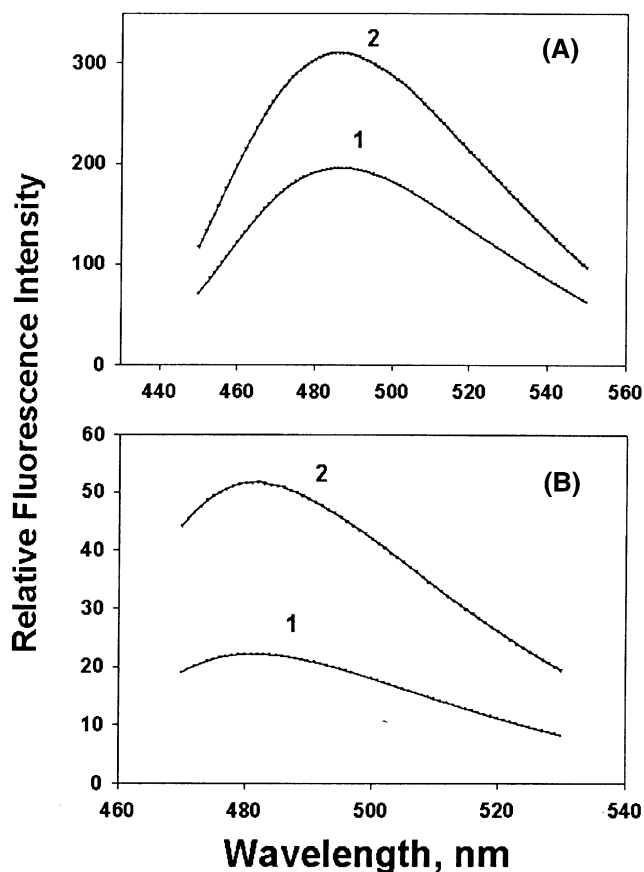


Fig. 6. (A) Bis-ANS and (B) ThT fluorescence spectra of native (curve 1) and HMW (curve 2) aggregated  $\alpha$ A-crystallins: Excitation wavelengths were 395 and 450 nm, respectively. Protein concentration was 0.1 mg/mL in 50 mM phosphate buffer, pH 7.4. Probe concentrations were 15  $\mu$ M for bis-ANS and 3  $\mu$ M for ThT.

and B). The results confirmed the earlier reports for a general tendency of increasing protein hydrophobicity in the HMW aggregates, regardless of whether the aggregation was induced by heat or was formed in vivo [2,3,6]. Increased ThT fluorescence can be attributed to an increased  $\beta$ -pleated sheet conformation as well as increased aggregation [3,20,21].

#### Subunit exchange

Fig. 7 shows the representative FRET spectra for the native and HMW aggregated  $\alpha$ A-crystallins mixed with MIANs-labeled W9F, showing decrease of Trp fluorescence intensity and increase of MIANs fluorescence intensity. This was possible because subunit exchange between MIANs-labeled W9F and WT  $\alpha$ A-crystallins brought the two probes in a close proximity. Fig. 8 shows FRET efficiencies with a function of time. The exchange was greater between the MIANs-labeled W9F  $\alpha$ A-crystallin mutant and the native  $\alpha$ A-crystallin than between the MIANs-labeled W9F  $\alpha$ A-crystallin mutant and the HMW aggregated  $\alpha$ A-crystallin.

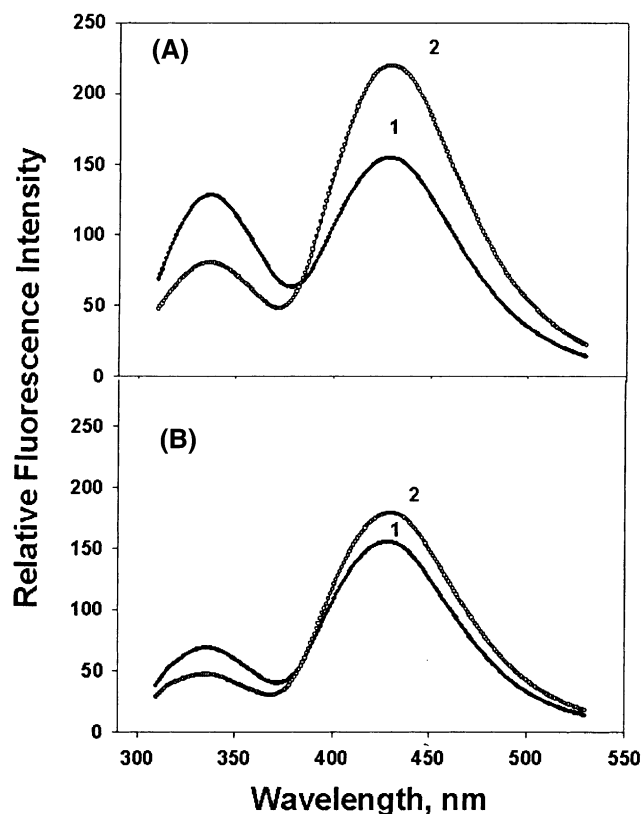


Fig. 7. FRET spectra for the native (A) and HMW aggregated (B)  $\alpha$ A-crystallins at 37  $^{\circ}$ C: curves 1 and 2 were at 0 and 6 h incubation, respectively. Equal amounts of unlabeled (HMW or control  $\alpha$ A-crystallin) and MIANs-labeled W9F  $\alpha$ A-crystallin samples (0.1 mg/mL) were mixed for the experiment.

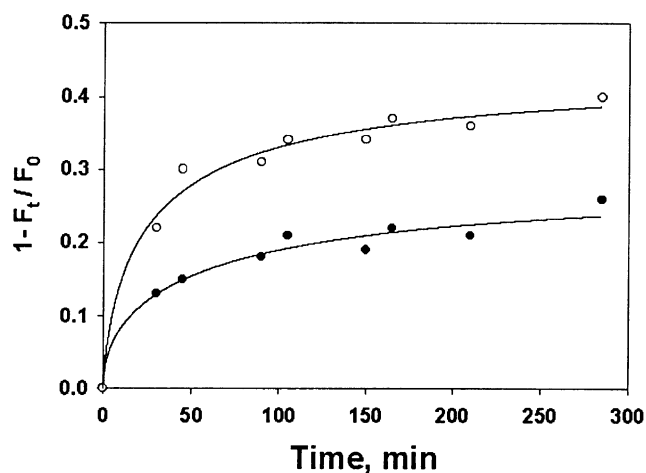


Fig. 8. FRET efficiencies for the native (○-○) and HMW aggregated (●-●)  $\alpha$ A-crystallins as a function of time at 37  $^{\circ}$ C. Each point was an average of two independent experiments.

#### Discussion

The irreversible changes of  $\alpha$ -crystallin brought about by heating have been previously established [2–5]. The

most noticeable change is HMW aggregation. The covalent change of disulfide formation detected in HMW aggregates has been thought to play a significant role in cataractogenesis. Our recent study using Cys-deficient  $\alpha$ A-crystallin mutants, however, indicates that disulfide cross-links contribute little to HMW aggregation [22]. In fact, HMW aggregation results from an initial partial unfolding and increased hydrophobic interaction. Partial unfolding exposed hydrophobic surfaces, which promotes hydrophobic interaction. The consequence is formation of HMW aggregates with a chain-like or filament structure [5,23]. Disulfide formation is more likely a result of partial unfolding that exposed buried cysteine groups.

The three-dimensional structure of  $\alpha$ -crystallin has not been determined, but many models have been proposed. Recently, a structural model was constructed on the basis of similarity in sequence between  $\alpha$ B-crystallin and *Mj* HSP16.5 [24,25]. The main feature is the presence of a hollow spherical structure, which is consistent with cryo-electron microscopic studies [26,27]. There may be two possible mechanisms for HMW aggregation: one involves partial disassembling and reassembling processes, in which the hollow spherical structure should be preserved, but no cryo-electron microscopy data were available. The other mechanism is association of partial unfolded proteins through hydrophobic interaction to form a filament- or chain-like structure, which has been observed in an electron microscopy study [5]. Our present data were unable to assign which structure, hollow or filament-like, was adopted by HMW aggregates.

The far-UV CD shows that the content of  $\beta$ -pleated sheet increased. This finding suggests that HMW aggregation was caused by stacking of increased  $\beta$ -pleated sheets. It is known that the side chains of amino acids that favor formation of  $\beta$ -pleated conformation are hydrophobic, such as valine and isoleucine [28]. We believe that HMW aggregation is caused by exposure of buried  $\beta$ -pleated sheets as well as by the increase of the percentage of  $\beta$ -pleated sheet.

One effect of HMW aggregation on  $\alpha$ -crystallin is reduced subunit exchange. This intersubunit exchange has been suggested to be responsible for stabilizing the protein during disturbance either from post-translational modifications or environmental changes [7]. However, disulfide formation and HMW aggregation may affect the intersubunit exchange. According to recent studies, exchange of subunits does not occur upon collision of two oligomers; rather it occurs through dissociation–reassociation of the oligomers [29,30]. Disulfide cross-linking and HMW aggregation will slow down the process and thus reduce the intersubunit exchange. This must have physiological relevance because HMW aggregation in the human lens may show the same adverse effects on the protein function.

In addition to its function as a structural protein,  $\alpha$ -crystallin was found to be a small heat-shock protein and could function as a chaperone [31]. It protects other crystallins from unfolding and aggregation. The effects of HMW aggregation on chaperone-like activity are different for in vitro and in vivo products. The HMW aggregates formed in vivo increase the chaperone activity and the heat-induced HMW aggregates decrease the activity [2,4,6,32]. The possible explanation is that in vivo HMW aggregation involves a lot of modifications that may offset the increased hydrophobicity due to partial unfolding. Modifications such as glycation, photooxidation, phosphorylation, deamidation, and mixed disulfide formation increase protein charge or hydrophilicity.

In conclusion, heat-induced HMW aggregation of  $\alpha$ -crystallin may result from partial unfolding and increased hydrophobic interaction. One major effect of HMW aggregation is a slower subunit exchange than the native protein, which may cause conformational instability.

## Acknowledgments

The work was supported by grants from the National Institutes of Health (EY05803) and Massachusetts Lions Eye Research Fund, Northborough MA.

## References

- [1] P.J. Groenen, K.B. Merck, W.W. de Jong, H. Bloemendal, Structure and modifications of the junior chaperone  $\alpha$ -crystallin. From lens transparency to molecular pathology, *Eur. J. Biochem.* 225 (1994) 1–19.
- [2] B.K. Das, J.J.N. Liang, B. Chakrabarti, Heat-induced conformational change and increased chaperone activity of lens  $\alpha$ -crystallin, *Curr. Eye Res.* 16 (1997) 303–309.
- [3] J.J.N. Liang, T.X. Sun, N.J. Akhtar, Heat-induced conformational change of human lens recombinant  $\alpha$ A- and  $\alpha$ B-crystallins, *Mol. Vis.* 6 (2000) 10–14.
- [4] K.P. Das, W.K. Surewicz, Temperature-induced exposure of hydrophobic surfaces and its effect on the chaperone activity of  $\alpha$ -crystallin, *FEBS Lett.* 369 (1995) 321–325.
- [5] M.R. Burgio, C.J. Kim, C.C. Dow, J.F. Koretz, Correlation between the chaperone-like activity and aggregate size of  $\alpha$ -crystallin with increasing temperature, *Biochem. Biophys. Res. Commun.* 268 (2000) 426–432.
- [6] J.J.N. Liang, N.J. Akhtar, Human lens high-molecular-weight  $\alpha$ -crystallin aggregates, *Biochem. Biophys. Res. Commun.* 275 (2000) 354–359.
- [7] P.J. van den Oetelaar, P.F. van Someren, J.A. Thomson, R.J. Siezen, H.J. Hoenders, A dynamic quaternary structure of bovine  $\alpha$ -crystallin as indicated from intermolecular exchange of subunits, *Biochemistry* 29 (1990) 3488–3493.
- [8] T.X. Sun, J.J.N. Liang, Intermolecular exchange and stabilization of human lens recombinant  $\alpha$ A- and  $\alpha$ B-crystallins, *J. Biol. Chem.* 273 (1998) 286–290.
- [9] M.P. Bova, L.L. Ding, J. Horwitz, B.K. Fung, Subunit exchange of  $\alpha$ A-crystallin, *J. Biol. Chem.* 272 (1997) 29511–29517.
- [10] T.X. Sun, N.J. Akhtar, J.J.N. Liang, Subunit exchange of lens  $\alpha$ -crystallin: a fluorescence energy transfer study with the fluorescent

- labeled  $\alpha$ -crystallin mutant W9F as a probe, *FEBS Lett.* 430 (1998) 401–404.
- [11] T.X. Sun, B.K. Das, J.J.N. Liang, Conformational and functional differences between recombinant human lens  $\alpha$ A- and  $\alpha$ B-crystallin, *J. Biol. Chem.* 272 (1997) 6220–6225.
- [12] P.K. Smith, R.I. Krohn, G.T. Hermanson, A.K. Mallia, F.H. Gartner, M.D. Provenzano, E.K. Fujimoto, N.M. Goetze, B.J. Olson, D.C. Klent, Measurement of protein using bicinchoninic acid, *Anal. Biochem.* 150 (1986) 76–80.
- [13] J.R. Lakowicz, *Principles of Fluorescence Spectroscopy*, Plenum Press, New York, 1983.
- [14] S.S. Gupte, L.K. Lane, Reaction of purified (Na,K)-ATPase with the fluorescent sulfhydryl probe 2-(4'-maleimidylanilino)naphthalene 6-sulfonic acid. Characterization and the effects of ligands, *J. Biol. Chem.* 254 (1979) 10362–10369.
- [15] U.P. Andley, J.N. Liang, B. Chakrabarti, Spectroscopic studies of lens crystallins. II. Fluorescence probes for polar–apolar nature and sulfhydryl group accessibility, *Biochemistry* 21 (1982) 1853–1857.
- [16] J.N. Liang, B. Chakrabarti, Spectroscopic studies of lens crystallins. I. Circular dichroism and intrinsic fluorescence, *Biochemistry* 21 (1982) 1847–1852.
- [17] O.P. Lamba, D. Borchman, S.K. Sinha, J. Shah, V. Renugopalakrishnan, M.C. Yappert, Estimation of the secondary structure and conformation of bovine lens crystallins by infrared spectroscopy: quantitative analysis and resolution by Fourier self-deconvolution and curve fit, *Biochim. Biophys. Acta* 1163 (1993) 113–123.
- [18] J.N. Liang, B. Chakrabarti, Intermolecular interaction of lens crystallins: from rotationally mobile to immobile states at high protein concentrations, *Biochem. Biophys. Res. Commun.* 246 (1998) 441–445.
- [19] L. Fu, J.J.N. Liang, Spectroscopic analysis of lens recombinant  $\beta$ B2- and  $\gamma$ C-crystallins, *Mol. Vis.* 7 (2001) 178–183.
- [20] H. Naiki, K. Higuchi, M. Hosokawa, T. Takeda, Fluorometric determination of amyloid fibrils in vitro using the fluorescent dye, thioflavin T1, *Anal. Biochem.* 177 (1989) 244–249.
- [21] J.J.N. Liang, Interaction between  $\beta$ -amyloid and lens  $\alpha$ B-crystallin, *FEBS Lett.* 484 (2000) 98–101.
- [22] S.J. Chen, T.X. Sun, N.J. Akhtar, J.J.N. Liang, Oxidation of human lens recombinant  $\alpha$ A-crystallin and cysteine-deficient mutants, *J. Mol. Biol.* 305 (2001) 967–976.
- [23] H.A. Kramps, A.L. Stols, H.J. Hoenders, On the quaternary structure of high-molecular-weight proteins from the bovine eye lens, *Eur. J. Biochem.* 50 (1975) 503–509.
- [24] K.K. Kim, R. Kim, S.H. Kim, Crystal structure of a small heat-shock protein, *Nature* 394 (1998) 595–599.
- [25] P.J. Muchowski, G. Wu, J.J.N. Liang, E.T. Adman, J.I. Clark, Site-directed mutation within the core “ $\alpha$ -crystallin” domain of the small heat-shock protein, human  $\alpha$ B-crystallin, diminish molecular chaperone functions, *J. Mol. Biol.* 289 (1999) 397–411.
- [26] D.A. Haley, J. Horwitz, P.L. Stewart, The small heat-shock protein,  $\alpha$ B-crystallin, has a variable quaternary structure, *J. Mol. Biol.* 277 (1998) 27–35.
- [27] J. Horwitz, M.P. Bova, L.L. Ding, D.A. Haley, P.L. Stewart, Lens  $\alpha$ -crystallin: function and structure, *Eye* 13 (1999) 403–408.
- [28] P.Y. Chou, G.D. Fasman, Empirical predictions of protein conformation, *Ann. Rev. Biochem.* 47 (1978) 251–276.
- [29] J. Vanhoudt, S. Abgar, T. Aerts, J. Clauwaert, Native quaternary structure of bovine  $\alpha$ -crystallin, *Biochemistry* 39 (2000) 4483–4492.
- [30] M.P. Bova, H.S. McHaourab, Y. Han, B.K. Fung, Subunit exchange of small heat shock proteins. Analysis of oligomer formation of  $\alpha$ A-crystallin and Hsp27 by fluorescence resonance energy transfer and site-directed truncations, *J. Biol. Chem.* 275 (2000) 1035–1042.
- [31] J. Horwitz,  $\alpha$ -Crystallin can function as a molecular chaperone, *Proc. Natl. Acad. Sci. USA* 89 (1992) 10449–10453.
- [32] L. Takemoto, D. Boyle, Molecular chaperone properties of the high molecular weight aggregate from aged lens, *Curr. Eye Res.* 13 (1994) 35–44.